Hot electron bolometer mixer for 20 - 40 THz frequency range

M.I. Finkel, S.N. Maslennikov, Yu.B. Vachtomin, S.I. Svechnikov
K.V. Smirnov, V.A. Seleznev, Yu.P. Korotetskaya, N.S. Kaurova, B.M. Voronov, and G.N. Gol'tsman
Moscow State Pedagogical University, Moscow, 119992, Russia, Email: goltsman@mspu-phys.ru

***Abstract*— The developed HEB mixer was based on a 5 nm thick NbN film deposited on a GaAs substrate. The active area of the film was patterned as a 30×20 μm^2 strip and coupled with a 50 Ohm coplanar line deposited *in situ*. An extended hemispherical germanium lens was used to focus the LO radiation on the mixer. The responsivity of the mixer was measured in a direct detection mode in the 25÷64 THz frequency range. The noise performance of the mixer and the directivity of the receiver were investigated in a heterodyne mode. A 10.6 μm wavelength CW CO_2 laser was utilized as a local oscillator.**

***Index Terms*—Superconducting radiation detectors, Hot carriers, Bollometers, Mixers.**

I. INTRODUCTION

The fact that the use of superconducting NbN hot electron bolometer (HEB) mixers has been planned for several widely known ground–based, stratosphere, and space–based platforms proves that their further improvement is the most promising for quantum limited terahertz heterodyne receivers at the frequencies above 1.3 THz. Indeed, it can be seen from fig. 1 that at these frequencies the most admissible noise performance is demonstrated by quasioptical or waveguide coupled NbN HEB mixers which show the values of the noise temperature close to $8\frac{hf_{LO}}{k}$, where f_{LO} is the local oscillator (LO) frequency. The use of a planar antenna or a waveguide in the mixer, on the one hand, enables us to decrease the volume and, consequently, to decrease the required LO power (to $\sim$ 1 μW) at the LO frequencies of several THz. On the other hand, it causes well known imperfections from which the most noticeable is the parasitic resistance of the contacts between the antenna and the sensitive NbN bridge (some improvement of the contacts has been achieved and reported in [1] recently), that becomes more essential when f_{LO} is increased. However, this imperfection can be eliminated by exclusion a separate antenna and, consequently, mentioned contacts from the mixer chip at all and making the sensitive bridge to be directly lens coupled. The reasonable dimensions for such a bridge are diffraction limited for certain value of f_{LO}. Although in most cases it means significant increase in the volume and, consequently, optimal LO power of the mixer, such a solution looks justified if we take into account that the requirements for the optimal LO power can be covered by recently developed quantum cascade lasers which can provide the power of $\sim$ 1 mW.

It should be noted that further experiments with NbN HEB mixers can provide an additional information and, consequently, can lead to a better understanding of the hot electrons and the heterodyne detection phenomena if the operating frequency significantly differs from conventional one for the antenna coupled mixers. The frequency range of 20÷40 THz looks the most reasonable for the first step experiments although at lower frequencies the performance of NbN HEB mixers may be better. In this frequency range, the NbN HEB mixers can be applied in space based planetary, solar and Earth science [28].

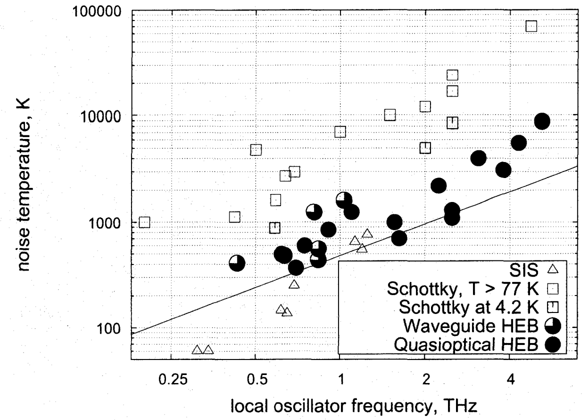

Fig. 1. Noise temperature (T_n) versus LO frequency (f_{LO}) and mixer type. Solid line corresponds to $T_n = 10\frac{hf_{LO}}{k}$. All the references for given graph are formated and shown below. The format is {<LO frequency, THz>, <noise temperature, K>, <reference>}. SIS: {0.31, 60, [2]}, {0.34, 60, [2]}, {0.618, 145, [3]}, {0.65, 136, [4]}, {0.69, 250, [5]}, {1.13, 650, [6]}, {1.2, 550, [7]}, {1.25, 760, [8]}. Schottky, $T \geqslant 77$ K: {0.2, 1000, [9]}, {0.42, 1120, [10]}, {0.5, 4800, [11]}, {0.59, 1608, [12]}, {0.64, 2720, [12]}, {0.69, 2970, [12]}, {1, 7100, [13]}, {1.5, 10000, [13]}, {2, 12000, [13]}, {2.5, 24000, [14]}, {2.5, 16800, [15]}, {4.750, 70000, [13]}. Schottky, $T \sim 4.2$ K: {0.585, 880, [16]}, {2.000, 5000, [17]}, {2.500, 8500, [13]}. Waweguide HEB: {0.430, 410, [18]}, {0.636, 483, [18]}, {0.810, 1250, [19]}, {0.840, 560, [19]}, {0.840, 440, [20]}, {1.035, 1600, [19]}. Quasioptical HEB: {0.620, 500, [21]}, {0.700, 370, [22]}, {0.750, 600, [23]}, {0.910, 850, [23]}, {1.100, 1250, [23]}, {1.560, 1000, [24]}, {1.620, 700, [25]}, {2.240, 2200, [24]}, {2.500, 1100, [25]}, {2.500, 1300, [26]}, {3.100, 4000, [27]}, {3.800, 3100, [26]}, {4.300, 5600, [27]}, {5.200, 8800, [27]}. .

The first results on characterization of the directly coupled NbN HEB mixers at the frequencies of 25÷60 THz are given below in sections "Fabrication process", "Characterization", and "Conclusions".

II. FABRICATION PROCESS

The key steps of the fabrication process are schematically shown in fig. 2.

A NbN/Au double–layer system is deposited on the epi–polished side of a semi–insulating GaAs substrate. Before the deposition the substrate is precleaned in acetone and isopropyl alcohol.

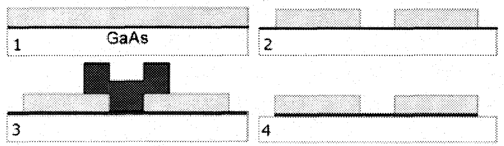

Fig. 2. The route of the structure processing. 1. NbN/Au double–layer system deposition on epi–polished side GaAs substrate. 2. Patterning of contact pads. 3. Patterning of sensitive bridge. 4. Chemical removal the NbN film outside of the bridge.

Ultrathin (5 nm) superconducting NbN film is deposited by dc reactive magnetron sputtering of Nb target in Ar and N_2 mixture in a Leybold Heraus Z–400 sputtering unit [29]. Residual pressure is $5{\cdot}10^{-7}$ mbar. During the NbN film deposition, the substrate is heated to 350 °C. The Ar partial pressure is $5{\cdot}10^{-3}$ mbar, and N_2 partial pressure is 10^{-4} mbar. The sputtering is carried out at a discharge current of 300 mA and a voltage of 400 V. A 100 nm thick Au film is then deposited *in situ* on the NbN film by dc magnetron sputtering at 100 °C. The parameters of the superconducting film are the following: the critical transition temperature is 9.4 K; superconducting transition width is 0.6 K; sheet resistance is 570 $\frac{\Omega}{\square}$ and ratio $R_{300}/R_{20} \sim 0.7$.

The layout is patterned by photolithography using a Karl Suss MA 56 mask aligner. At first the contact pads are formed, and then the topology of the sensitive bridge ($30{\times}20\ \mu m^2$) is patterned.

At the last stage the GaAs substrate is scribed into the chips ($3{\times}3\ mm^2$) that are cleaned in acetone to strip the photoresist. One of the chips prepared is shown in fig. 3. Although the NbN film thickness is no more than 5 nm, the sensitive element appears as a mesa–structure caused by high etching rate of GaAs during the NbN film removal process.

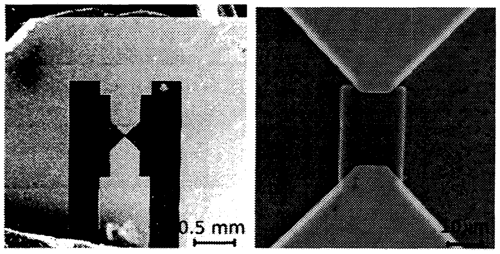

Fig. 3. SEM photos of directly lens coupled NbN HEB mixer.

III. CHARACTERIZATION

A. Noise performance

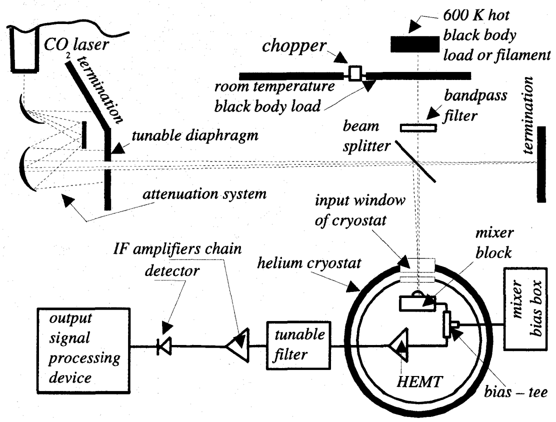

Fig. 4. Experimental setup.

The experimental setup for the noise performance characterization of directly lens coupled NbN HEB mixers is shown in fig. 4. As a local oscillator (LO) a 10.6 μm wavelength CW CO_2 discharge laser is used. Its radiation power is attenuated and focused by a system consisting of two off–axis mirrors, several black body terminations and a handled diaphragm. In order to superimpose the radiations of LO and a signal source a beam splitter is used. Signal source (600 K black body or 1200 K filament, T_h) radiation is chopped with a room temperature T_{cold} black body load. A liquid helium cryostat equiped by a Ge input window is utilized to cool the mixer to its operating temperature (4.2 K). The mixer block includes Ge extended hemispherical lens (diameter $D \sim 12$ mm, extension lenght $\sim \frac{1}{6}D$) with a mixing device positioned on the flat surface side. The intermediate frequency signal is guided out of the chip via a 50 Ohm coplanar line which is soldered to an SMA connector. A bias tee is used to feed the bias to the mixer and to transmit the intermediate frequency signal to low noise (noise temperature of ~ 6 K) HEMT amplifier (1.3÷1.9 GHz). The output signal is detected by a broadband microwave detector and processed for Y–factor calculation.

It should be noted that for the noise temperatures close to the quantum limit the term correspondent to the zero fluctuations (quantum) noise is not negligible in the expression for Y–factor:

$$Y = \frac{\frac{1}{k}D(f_{LO}, T_h) + \frac{hf_{LO}}{2k} + T_n^{CW}}{\frac{1}{k}D(f_{LO}, T_{cold}) + \frac{hf_{LO}}{2k} + T_n^{CW}} \tag{1}$$

where T_n^{CW} is the receiver's equivalent noise power per unit bandwidth divided by k given at the input (*receiver's Callen & Welton noise temperature* [30]), and

$$D(\nu, T) = \frac{h\nu}{e^{\frac{h\nu}{kT}} - 1} \tag{2}$$

is the radiation spectral density of the black body load at a frequency of ν and a temperature of T.

In the experiments, the values of the Y–factor were measured at the setup described above using both a ~ 1200 K filament and 600 K black body loads, and then the values of T_n^{CW} were calculated for several operating points (fig. 5). For the optimal operating point the values of T_n^{CW} are shown

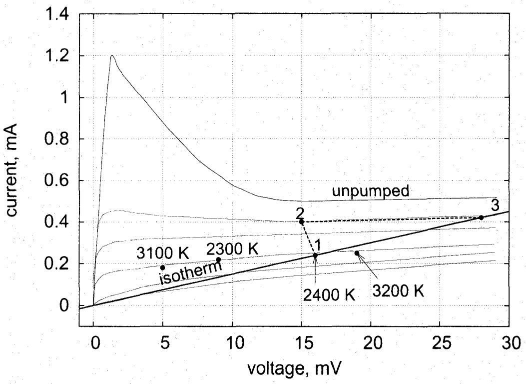

Fig. 5. IV–curves and several values of the noise temperature given at the points near the optimal IV–curve.

TABLE I

DEPENDENCE OF Y-FACTOR AND NOISE TEMPERATURE VERSUS TEMPERATURE OF HOT LOAD T_h.

T_h, K	Y	T_n^{CW}, K
600	1.06	2300
1200	1.2	2400

in table I.

It should be noted that, due to significant increase in the device volume, the contribution of the effect of direct detection to the value of the output signal [26], [31] was negligibly small and, consequently, could not appreciably distort the values of T_n^{CW}.

B. Optimal LO power

So called *isothermal method* was applied to estimate the value of the optimal LO power absorbed. In particular, for the point 1 (close to optimal one, fig. 5), LO power absorbed was deduced from the equations (3) and (4). As the resistances at the points 1 and 3 (fig. 5) are equal, for the electron temperatures at these points it should be true that $T_1^e = T_3^e$, and consequently, for LO powers absorbed P_1^{LO}, P_3^{LO}, bias voltages U_1, U_3 and currents I_1, I_3 it can be written:

$$P_1^{LO} + U_1 I_1 = P_3^{LO} + U_3 I_3 \tag{3}$$

The transition from point 1 to point 2 is done by 3 dB attenuation of the LO power, that gives another equation:

$$P_1^{LO} \simeq 2P_2^{LO} \simeq 2P_3^{LO} \tag{4}$$

From (3) and (4) the estimated value of the absorbed LO power at the operating point close to the optimal one is $P_1^{LO} \simeq 16$ μW.

C. Receiver's beam pattern

The beam pattern of the mixer+lens system was measured in the heterodyne mode with a chopped 1200 K filament as a signal radiation source. The result is shown in fig. 6. It can be seen that beam pattern obtained is essentially narrower than that of mixer—log-spiral—lens antenna system at 2.5 THz [32] (dotted line in fig. 6).

D. Receiver's responsivity versus frequency

The responsivity of the receiver was investigated in the detection mode using a chopped filament and a room temperature black body as the signal loads which radiated a power dP per solid angle dΩ, area dS_{bb}, and bandwith dν of

$$\frac{\mathrm{d}P}{\mathrm{d}S_{bb}\mathrm{d}\Omega\mathrm{d}\nu} \simeq \left(\frac{2h\nu^3}{c^2}\right)\frac{1}{e^{\frac{h\nu}{kT}}-1} \equiv \mathcal{D}_{S\Omega\nu}(\nu,T) \tag{5}$$

(here T was the temperature of correspondent load). In the case when both the angle α and solid angle Ω (fig. 7) are small ($S_l \ll l^2$, $S_{bb} \ll l^2$, where S_l is the area of the input diaphragm mounted in the cryostat in front of Ge lens) the expression for the incident power per unit bandwidth can be written as

$$\begin{aligned}\frac{\mathrm{d}P}{\mathrm{d}\nu} &\simeq \mathcal{D}_{S\Omega\nu}(\nu,T)\cdot S_{bb}\cdot\Omega = \\ &= \left(\frac{\alpha^2 S_l \pi h\nu^3}{2c^2}\right)\frac{1}{e^{\frac{h\nu}{kT}}-1} \equiv \mathcal{D}_\nu(\nu,T)\end{aligned} \tag{6}$$

In order to obtain a rough dependence of the receiver's responsivity versus frequency a set of bandpass dispersion filters was used (fig. 4, 8). For certain filter the responsivity can be deduced using (6) and expressed as:

$$s \simeq \frac{U_r}{\int_0^\infty \mathcal{T}(\nu)\left(\mathcal{D}_\nu(\nu,T_{bb}) - \mathcal{D}_\nu(\nu,T_r)\right)\mathrm{d}\nu} \tag{7}$$

where $\mathcal{T}(\nu)$ is the dependence of the filter transmission versus frequency, $T_r \simeq 296$ K and $T_{bb} \simeq 1200$ K are the room and filament temperatures, respectively, and U_r is the response voltage.

In the experiments, U_r was measured by a lock–in amplifier for each filter of the set, and then the responsivity was calculated using (7) (fig. 8). It can be concluded that at the frequencies $\lesssim 30$ THz the device responsivity is cut by Ge input window of the cryostat and the lens, while at the frequencies $\gtrsim 30$ THz the responsivity is almost flat and close to 70 $\frac{V}{W}$.

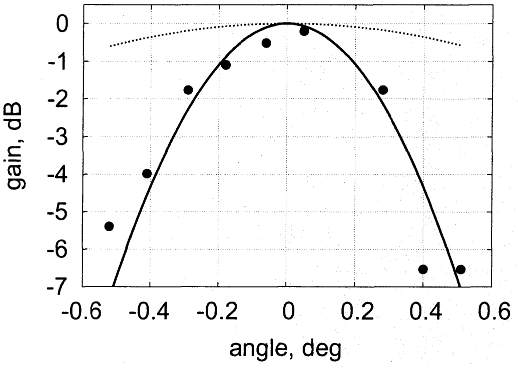

Fig. 6. Receiver's beam pattern. Dotted line corresponds to the beam pattern of the system consisting of Si lens, spiral antenna and mixer at 2.5 THz [32].

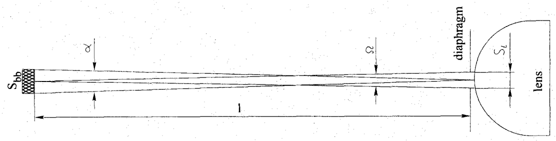

Fig. 7. Denotations for a black body load and the input diaphragm mounted in the cryostat in front of Ge lens.

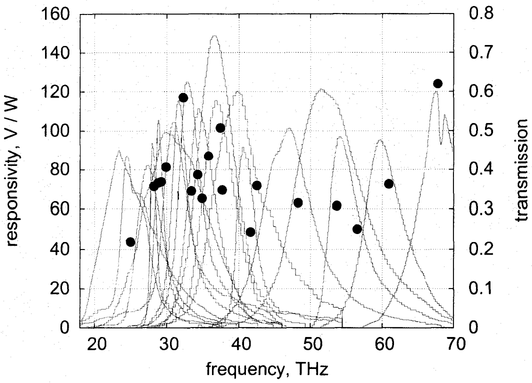

Fig. 8. The dependence of the receiver's responsivity versus frequency (filled circles) and the transmissions of the bandpass filters used in the experiment (lines).

IV. Conclusions

At high frequencies directly lens coupled NbN HEB mixer shows lower noise temperature than antenna coupled one. First experiment with NbN HEB at 30 THz gives the noise temperature about 2300 K that is close to 3 times of the quantum limit. For the 30×20 μm^2 device the optimal absorbed LO power is about 16 μW that is relatively easy to get from solid state sources in the middle IR. The responsivity of the device versus frequncy is almost flat and is about 70 $\frac{V}{W}$ in the frequency range of 25÷60 THz.

References

[1] J. Baselmans, M. Hajenius, J. Gao, T. Klapwijk, P. de Korte, B. Voronov, and G. Gol'tsman, "Doubling of sensitivity and bandwidth in phonon cooled hot electron bolometer mixers," *Appl. Phys. Lett.*, no. 84, p. 1958, 2004.

[2] S. Claude, "Sideband-Separating SIS Mixer For ALMA Band 7, 275–370 GHz," in *Proc. 14th international symphosium on space terahertz technology*, Tucson, USA, Mar. 2003, p. 41.

[3] S. Shi, C. Chin, M. Wang, W. Shan, W. Zhang, and T. Noguchi, "Development of a 600–720 GHz SIS Mixer for the SMART," in *Proc. 12th international symphosium on space terahertz technology*. San Diego, CA, USA: Jet Propulsion Laboratory, California Institute of Technology, Feb. 2001, p. 215.

[4] A. Baryshev, E. Lauria, R. Hesper, T. Zijlstra, and W. Wild, "Fixed-tuned waveguide 0.6 THz SIS mixer with Wide band IF," in *Proc. 13th international symphosium on space terahertz technology*. Cambridge, MA, USA: Harward University, Mar. 2002.

[5] P. Grimes, P. Kittara, G. Yassin, S. Withington, and K. Jacobs, "Investigation of the performance of a 700 GHz nline mixer," in *Proc. 14th international symphosium on space terahertz technology*, Tucson, USA, Mar. 2003, p. 247.

[6] A. Karpov, D. Miller, F. Rice, J. Zmuidzinas, J. Stern, B. Bumble, and H. LeDuc, "Low noise 1.2 THz SIS receiver," in *Proc. 12th international symphosium on space terahertz technology*. San Diego, CA, USA: Jet Propulsion Laboratory, California Institute of Technology, Feb. 2001, pp. 21–22.

[7] A. Karpov, D. Miller, F. R. Rice, J. A. Stern, B. Bumble, H. G. LeDuc, and J. Zmuidzinas, "Low–noise SIS mixer for far–infrared radio astronomy," in *Proc. SPIE*, vol. 5498, Glasgow, Scotland, UK, June 2004, pp. 616–621.

[8] A. Karpov, D. Miller, J. A. Stern, B. Bumble, H. G. LeDuc, and J. Zmuidzinas, "Low noise NbTiN 1.25 THz SIS mixer for Herschel Space Observatory," in *Abstract Book – ISSTT 2005*, Göteborg, Sweden, May 2005, p. 159.

[9] I. Galin, C. Schnitzer, R. Dengler, and O. Quintero, "177-207 GHz Radiometer Front End, Single–Side–Band Measurements," in *Proc. 10th international symphosium on space terahertz technology*, Charlotte Sville, Virginia, Mar. 1999, p. 70.

[10] J. L. Hesler, K. Hui, and T. W. Crowe, "A Fixed–tuned 400 GHz Subharmonic Mixer Using Planar Schottky Diods," in *Proc. 10th international symphosium on space terahertz technology*, Charlotte Sville, Virginia, Mar. 1999, p. 95.

[11] B. Maddison, R. Martin, M. Oldfield, C. Mann, D. Matheson, B. Ellison, J. Thornton, W. Hall, and D. Lamarre, "A Compact 500 GHz Planar Schottky Diode Receiver with a Wide Instantaneous Bandwidth," in *Proc. 9th international symphosium on space terahertz technology*, 1998, p. 367.

[12] S. M. Marazita, K. Hui, J. L. Hesler, W. L. Bishop, and T. W. Crowe, "Progress in submillimeter wavelength integrated mixer technology," in *Proc. 10th international symphosium on space terahertz technology*, Charlotte Sville, Virginia, Mar. 1999, p. 74.

[13] A. Betz and R. Borejko, "A practical Schottky mixer for 5 THz," in *Proc. 7th international symphosium on space terahertz technology*, 1996, p. 503.

[14] T. Suzuki, C. Mann, T. Yasui, H. Fujishima, and K. Mizuno, "Quasi–integrated planar Schottky barrier diodes for 2.5 THz receivers," in *Proc. 9th international symphosium on space terahertz technology*, 1998, p. 187.

[15] C. Mann, D. Matheson, B. Ellison, M. Oldfield, B. Moyna, J. Spencer, D. Wilsher, and B. Maddison, "On the design and measurement of a 2.5 THz waveguide mixer," in *Proc. 9th international symphosium on space terahertz technology*, 1998, p. 161.

[16] J. Hesler, W. Hall, T. Crowe, R. Weikle, R. Bradley, and Shing–Kuo Pan, "Submm wavelenght waveguide mixers using planar Schottky barier diods," in *Proc. 7th international symphosium on space terahertz technology*, 1996, p. 462.

[17] *Millimeter and Submillimeter Techniques*, , W. Ross Stonel ed., ser. Review of radio science 1993–1996. New York: Oxford University Press Inc, 1996.

[18] J. Kawamura, R. Blundell, C–Y.E. Tong, G. Gol'tsman, E. Gershenzon, B. Voronov, and S. Cherednichenko, "Phonon–cooled NbN HEB Mixers for Submillimeter Wavelengths," in *Proc. 8th international symposium on space terahertz technology*, Mar. 1997, p. 23.

[19] C.-Y. Edward Tong, J. Kawamura, T. R. Hunter, D. C. Papa, R. Blundell, M. Smith, F. Patt, G. Gol'tsman, and E. Gershenzon, "Successful operation of a 1 THz NbN hot–electron bolometer receiver," in *Proc. 11th international symphosium on space terahertz technology*, May 2000, pp. 49–59.

[20] D. Loudkov, C.-Y. Tong, R. Blundell, N. Kaurova, E. Grishina, B. Voronov, and G. Gol'tsman, "An investigation of the performance of the superconducting HEB mixer as a function of its RF embedding impedance," T, lo be published in ASC 2004 proc.

[21] P. Yagoubov, M. Kroug, H. Merkel, E. Kollberg, J. Shubert, H. Hübers, S. Svechnikov, B. Voronov, G. Gol'tsman, and Z. Wang, *Supercond. Sci. Technol.*, no. 12, 1999.

[22] K. Smirnov, Y. Vachtomin, S. Antipov, S. Maslennikov, N. Kaurova, V. Drakinsky, B. Voronov, G. Gol'tsman, A. Semenov, H.-W.Hübers, and H. Richter, "Noise performance of spiral antenna coupled HEB mixers at 0.7 THz and 2.5 THz," in *Proc. 14th international symphosium on space terahertz technology*, Tucson, USA, Mar. 2003.

[23] R. Wyss, B. Karasik, W. McGrath, B. Bamble, and H. LeDuc, "Noise and bandwidth measurements of diffusion–cooled Nb hot–electron bolometer mixers at frequencies above the superconductive energy gap," in *Proc. 10th international symphosium on space terahertz technology*, Charlotte Sville, Virginia, Mar. 1999, pp. 215–229.

[24] E. Gerecht, C. Musante, H. Jian, Y. Zhuang, K. Yngvesson, J. Dickinson, T. Goyette, J. Waldman, P. Yagoubov, G. Gol'tsman, B. Voronov, and E. Gershenzon, "Improved characteristics of NbN HEB mixers integrated with log–periodic antennas," in *Proc. 10^{th} international symphosium on space terahertz technology*, Charlotte Sville, Virginia, Mar. 1999, pp. 200–207.

[25] M. Kroug, S. Cherednichenko, H. Merkel, E. Kollberg, B. Voronov, G. Gol'tsman, H.-W. Hübers, and H. Richter, Presented at the Applied Superconductivity Conference, Virginia Beach, USA (to be published in the IEEE Transactions on Applied Superconductivity), 2000.

[26] Y. Vachtomin, S. Antipov, S. Maslennikov, K. Smirnov, S. Polyakov, N. Kaurova, E. Grishina, B. Voronov, and G. Gol'tsman, "Noise temperature measurements of NbN phonon–cooled hot electron bolometer mixer at 2.5 and 3.8 THz," in *Proc. 15^{th} international symphosium on space terahertz technology*, Northampton, Massachusetts, USA, Apr. 2004.

[27] J. Schubert, A. Semenov, G. Gol'tsman, H.-W. Hübers, G. Schwaab, B. Voronov, and E. Gershenzon, *Supercond. Sci. Technol.*, no. 12, p. 748, 1999.

[28] T. Kostiuk, "Heterodyne spectroscopy in the thermal infrared region: a window on physics and chemistry," in *Proc. International Thermal Detectors Workshop (TDW'03), session 7 (Heterodyne detectors)*. 3501 University Boulevar East Adelphi, MD 20783: University of Maryland Inn and Conference Center, June 2003.

[29] P. Yagubov, G. Gol'tsman, B. Voronov, L. Seidman, V. Siomash, S. Cherednichenko, and E. Gershenzon, "The bandwidth of HEB mixers employing ultrathin NbN films on sapphire substrate," in *Proc. 7^{th} international symposium on space terahertz technology*, Charlottesville, Virginia, USA, Mar. 1996, pp. 290–302.

[30] A. Kerr, M. Feldman, and S.–K. Pan, "Receiver noise temperature, the quantum noise limit, and zero–point fluctuations," in *Proc. 8^{th} international symposium on space terahertz technology*, Mar. 1997, pp. 101–111.

[31] J. Baselmans, A. Baryshev, S. Reker, M. Hajenius, J. Gao, T. Klapwijk, Y. Vahtomin, S. Maslennikov, S. Antipov, B. Voronov, and G. Gol'tsman, "Direct detection effect in small volume hot electron bolometer mixers," *Appl. Phys. Lett.*, no. 86, p. 163503, 2005.

[32] A. Semenov, Heinz.–Wilhelm Hübers, H. Richter, M. Birk, M. Krocka, U. Mair, K. Smirnov, G. Gol'tsman, and B. Voronov, "Performance of terahertz heterodyne receiver with a superconducting hot–electron mixer," in *Proc. 13^{th} international symphosium on space terahertz technology*. Cambridge, MA, USA: Harward University, Mar. 2002, pp. 229–234.